




Synthesis, characterization and medical efficacy (hepatoprotective and antioxidative) of albendazole-based copper(II) complexes – an experimental and theoretical approach

Mohamed M. Ibrahim, Abdel-Motaleb M. Ramadan, Hamdy S. El-Sheshtawy, Mahmoud A. Mohamed, Mohamed Soliman & Sayed I.M. Zayed


To cite this article: Mohamed M. Ibrahim, Abdel-Motaleb M. Ramadan, Hamdy S. El-Sheshtawy, Mahmoud A. Mohamed, Mohamed Soliman & Sayed I.M. Zayed (2015) Synthesis, characterization and medical efficacy (hepatoprotective and antioxidative) of albendazole-based copper(II) complexes – an experimental and theoretical approach, Journal of Coordination Chemistry, 68:24, 4296-4313, DOI: [10.1080/00958972.2015.1093124](https://doi.org/10.1080/00958972.2015.1093124)


To link to this article: <http://dx.doi.org/10.1080/00958972.2015.1093124>

 View supplementary material 

 Accepted author version posted online: 15 Sep 2015.
Published online: 19 Oct 2015.

 Submit your article to this journal 

 Article views: 50

 View related articles 

 View Crossmark data 

Synthesis, characterization and medical efficacy (hepatoprotective and antioxidative) of albendazole-based copper(II) complexes – an experimental and theoretical approach

MOHAMED M. IBRAHIM^{*†‡}, ABDEL-MOTALEB M. RAMADAN[†],
HAMDY S. EL-SHESHTAWY[†], MAHMOUD A. MOHAMED[§],
MOHAMED SOLIMAN^{‡¶} and SAYED I.M. ZAYED^{‡¹}

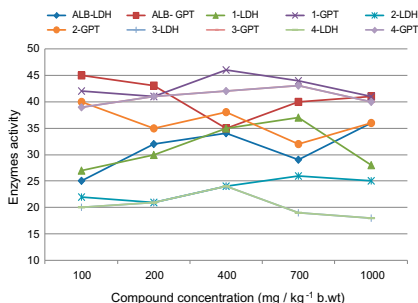
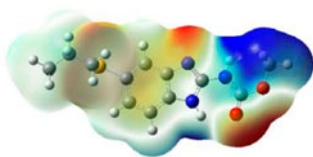
[†]Faculty of Science, Department of Chemistry, Kafr El-Sheikh University, Kafr El-Sheikh, Egypt

[‡]Faculty of Science, Department of Chemistry, Taif University, Taif, Saudi Arabia

[§]Faculty of Agriculture, Department of Biochemistry, Cairo University, Cairo, Egypt

[¶]Faculty of Veterinary Medicine, Department of Biochemistry, Benha University, Benha, Egypt

(Received 21 February 2015; accepted 14 August 2015)



A series of albendazole-based copper(II) complexes with different counter anions, $[\text{Cu}(\text{Albz})(\text{H}_2\text{O})_2](\text{ClO}_4)_2$ (**1**), $[\text{Cu}(\text{Albz})_2(\text{Cl})]\text{Cl} \cdot 2\text{H}_2\text{O}$ (**2**), $[\text{Cu}(\text{Albz})_2(\text{NO}_3)](\text{NO}_3)$ (**3**), and $[\text{Cu}_2(\text{Albz})_2(\mu\text{-SO}_4)_2(\text{H}_2\text{O})_2]$ (**4**) (Albz = albendazole), have been synthesized and characterized. Their structures and properties were characterized by elemental analysis, thermal analysis (TGA, DTG and DTA), IR, UV–vis and ESR spectroscopies, cyclic voltammetry, electrical molar conductivity, and magnetic moment measurements. A square-planar geometry is proposed for **1**, whereas the five-coordinate copper(II) complexes **2**, **3**, and **4** have a square pyramidal geometry. Theoretical calculations (DFT) using B3LYP/6–311 + G(d,p) level of theory corroborated the experimental results to investigate both the drug Albz and its copper(II) complex, **1**. The hepatoprotective and antioxidative efficacy of Albz and **1–4** were evaluated against carbon tetrachloride-induced acute hepatotoxicity in rats. Hepatotoxicity in experimental rats was evidenced by significant decrease in the antioxidant enzyme activities (SOD, GSH-S-transfers, and GSH-Rd levels). The results have strong impact for designing anticancer drugs, combined with their potential cytotoxic and antioxidant activities, which can be targeted selectively against cancer cells and increase their therapeutic index and advantages over other anticancer drugs. The DNA cleavage studies of Albz and its copper(II) complexes using

*Corresponding author. Email: ibrahim652001@yahoo.com

¹Present address: Faculty of Industrial Education, Beni-Suef University, Beni-Suef, Egypt.

genomic DNA indicated that Albz has no role in cleavage of DNA, and only **1** played a marked role in the DNA cleavage without any external additives.

Keywords: Albendazole; Copper(II) complexes; Spectroscopy; Enzymatic antioxidants; DNA cleavage

1. Introduction

Free radicals in the form of reactive oxygen and nitrogen species are an integral part of normal physiology. Overproduction of these reactive species can occur due to oxidative stress brought about by imbalance of the bodily antioxidant defense system and free radical formation. These reactive species can react with biomolecules, causing cellular injury and even death [1]. The majority of diseases are linked to oxidative stress due to free radicals. Free radicals are fundamental to any biochemical process and represent an essential part of aerobic life and metabolism. Free radical oxidative stress has been implicated in the pathogenesis of a wide variety of clinical disorders, such as cancer, cardiovascular disease, Alzheimer, autoimmune diseases, diabetes, multiple sclerosis, and arthritis [2].

Free radicals are produced by radiation or as by-products of metabolic processes. They initiate chain reactions, which lead to disintegration of cell membranes and cell compounds, including lipids, proteins, and nucleic acids [3]. Biological systems protect themselves against the damaging effects of activated species by several means, including free radical scavengers and chain reaction terminators and enzymes, such as SOD and CAT system [4]. If human disease is due to imbalance between oxidative stress and antioxidative defense, it is possible to limit oxidative tissue damage and hence prevent disease progression of antioxidant defense supplements [5]. If the balance sways in the direction of pro-oxidants, oxidative stress can arise, but under normal circumstances is controlled by a broad range of antioxidant enzymes, proteins, and antioxidants provided by the diet.

Consumption of fruits and vegetables [6] containing antioxidants offers protection against these diseases. Antioxidants are often added to foods to prevent the radical chain reactions of oxidation, and they act by inhibiting the initiation and propagation step leading to the termination of the reaction and delay of the oxidation process [7].

It is a general aim of modern catalysis to develop substances that are able to act as highly active and selective catalysts. In order to achieve this goal, various approaches may be tried. One of the most promising ways is attempting to mimic nature's most efficient catalysts, the enzymes [8]. Study of structural models increases understanding of fundamental mechanistic aspects of enzymes as well as development of structure reactivity relationships [9–15]. The major task in designing these model compounds depends on proper choice of ligands as well as the stereochemical environment surrounding the metal centers.

Imidazole nitrogen donors of histidyl residues are the most common binding sites in various metalloenzymes [16]. Therefore, ligands containing imidazole or benzimidazole rings can potentially mimic the binding sites and catalytic activities of enzymes. The ligand albendazole (Albz) is a bidentate NO donor with donor groups suitably placed for forming a six-membered chelate ring.

The goal of the present study was to examine the antioxidant and hepatoprotective activity of four new albendazole-based copper(II) complexes with different counter anions, $[\text{Cu}(\text{Albz})(\text{H}_2\text{O})_2](\text{ClO}_4)_2$ (**1**), $[\text{Cu}(\text{Albz})_2(\text{Cl})]\text{Cl}\cdot 2\text{H}_2\text{O}$ (**2**), $[\text{Cu}(\text{Albz})_2(\text{NO}_3)](\text{NO}_3)$ (**3**),

and $[\text{Cu}_2(\text{Albz})_2(\mu\text{-SO}_4)_2(\text{H}_2\text{O})_2]$ (**4**) (Albz = albendazole) against oxidative stress induced by CCl_4 in rats. DNA cleavages of Albz and its copper(II) complexes using genomic DNA were also examined.

2. Experimental

Caution: Salts of perchlorate and their metal complexes are potentially explosive and should be handled with great care and in small quantities.

2.1. Materials and general methods

The Albz was purchased from Merck Chemical Company (purity/analysis > 98%) and used without purification. Dimethyl sulfoxide (DMSO), carbon tetrachloride (CCl_4), and vitamin E were obtained from Sigma Chemical Co. (St. Louis, MO, USA). All enzymatic kits were purchased from Bioassays system, USA. IR spectra were recorded using an Alpha-Atunated FT-IR Spectrophotometer, Bruker from 400–4000 cm^{-1} . All UV–vis measurements were recorded by a UV-Lambda 25 Perkin Elmer. Magnetic moments were measured by Gouy's method at room temperature. ESR measurements of polycrystalline samples at room temperature were taken on a Varian E9 X-band spectrometer using a quartz Dewar vessel. All spectra were calibrated with DPPH ($g = 2.0027$). The specific conductances of the complexes were measured using freshly prepared (10^{-3} M) aqueous solutions at room temperature using a YSI Model 32 conductance meter. Thermal analyses of the complexes were recorded on a Netzsch STA 449F3 with system interface device in the atmosphere of nitrogen. The temperature scale of the instrument was calibrated with high purity calcium oxalate. The operational range of the instrument was from ambient temperature to 1400 °C. Pure sample (15 mg) was subjected for dynamic TG scans at heating rate of 20 °C min^{-1} .

2.2. Synthesis of the copper(II) complexes 1–4

The reported copper(II) complexes **1–4** were prepared by mixing methanolic solution of Albz (265 mg, 1.0 mmol) with the corresponding copper(II) salts in 1 : 1 M ratio. After 30 min stirring at room temperature, the chelation reaction was completed and the complexes precipitated. In each case, the formed microcrystalline product was filtered off, washed several times with cold alcohol, ether, and finally dried under vacuum over anhydrous CaO .

2.3. Computational details

All calculations were performed by the Gaussian03 program. Ground state geometries were calculated using Kohn-Sham density functional theory (DFT) with the Becke3-Lee-Yang-Parr hybrid functional (B3LYP) method using the 6-311 + G (d,p) basis set for full structural optimization and frequency calculations. Analytical frequency calculations were done in order to verify the stationary points on the potential energy surface. Exclusively positive frequencies and no imaginary negative frequencies for the energy minima were found. To

calculate excitation energies, time-dependant density functional theory calculations (TD-DFT) were also conducted at the B3LYP/6–311 + G(d,p) level of theory.

2.4. Electrochemical measurements

The cyclic voltammetric measurements were performed using Metrohm 797 VA Computrace (Herisau, Switzerland) equipped with a Metrohm VA 694 stand. Three electrode assembly cells consisted of carbon paste electrode (CPE) as working electrode, Ag/AgCl in 0.03 M KCl as a reference electrode and platinum wire as an auxiliary electrode.

2.5. Biological experiments

2.5.1. Experimental animals. Male Albino mice (25 ± 5 g) were obtained from the Department of Animal Science, Cairo University. Animals were handled under standard laboratory conditions and maintained with a 12-h light/dark cycle at 25 ± 5 °C and relative humidity of $55 \pm 5\%$ controlled room. The basal diet used in this study was certified fed to research laboratory animals at Cairo University. Food and water were available *ad libitum*. The committee of animal care and use at Cairo University approved all protocols carried out on animals used in this study.

2.5.2. Toxicity experiment. The toxicities of **1–4** were evaluated in animal system by different biochemical profiles, including LD₅₀ (the amount required to kill 50% of a given test population), activities of GPT (Glutamate pyruvate transaminase) and LDH (lactate dehydrogenase). Ninety-eight male albino mice weighing 25 ± 5 g were used for this experiment and divided into 14 groups (7 mice per group). Mice were injected after overnight fasting with graded doses of 100–1000 mg kg^{−1} b.wt., intraperitoneally (i.p) of synthesized compounds suspended in DMSO. The toxicological effects were observed after 72 h of treatment in terms of mortality and expressed as LD₅₀ [17]. Other biochemical parameters were determined after 14 days of administration according to methods of Reitman and Frankel [18] for GPT activity and Bergmeyer [19] for LDH activity.

2.5.3. Bioassays and experimental design. Hepatoprotective and antioxidant activity of Albz and **1–4** were evaluated against CCl₄-induced acute hepatotoxicity in mice. The animals were randomly divided into 14 groups of 5 mice per group. The first group served as normal control received vehicle only (propylene glycol, 5 mL kg^{−1} b.wt. per day intragastric). Group 2 received single dose of equal mixture of CCl₄ and olive oil (50%, v/v, 0.5 mL kg^{−1} b.wt. i.p) and served as infected control group. Groups from 3 to 12 were pretreated with individual synthesized compounds at 100 and 300 mg kg^{−1} b.wt. per day intragastric, respectively, for 7 days. On the seventh day, equal mixture of CCl₄ and olive oil (50%, v/v, 0.5 mL kg^{−1} b.wt. i.p.) was administrated orally [20]. Group 14 was pretreated with standard drug Vitamin E (100 mg kg^{−1} b.wt. per day intragastric) for 7 days. Twenty-four hours after the last administration, mice were sacrificed after dimethyl ether inhalation. Blood samples were collected and centrifuged at $4000 \times g$ at 4 °C for 10 min for serum extraction. The liver was removed rapidly, washed and homogenized in ice-cold physiological saline to prepare 10% (w/v) homogenate. Then, the homogenate was centrifuged at

4000 \times g at 4 °C for 10 min to remove cellular debris, and the supernatant was collected for biochemical assays.

2.5.4. Biochemical assays. Glutathione-S-Transferase (GST) activity was determined as described by Habig *et al.* [21]. Reaction mixture contained 50 mM phosphate buffer, pH 7.5, 1.0 mM of 1-chloro-2,4-dinitrobenzene (CDNB), and an appropriate volume of compound solution. The reaction was initiated by addition of reduced glutathione (GSH) and formation of S-(2,4-dinitro phenyl) glutathione (DNP-GS) was monitored as an increase in absorbance at 334 nm. The result was expressed as μ mol of CDBN conjugation formed/mg protein/min. Superoxide dismutase (SOD) activity was measured through the inhibition of hydroxylamine oxidation by the superoxide radicals generated in the xanthine–xanthine oxidase system [22]. The results were expressed in units/mg protein. *Glutathione Reduced (GSH-Rd)* in liver and kidney tissues was determined according to the Ellman method [23], which measures the reduction of 5,50-dithio-bis(2-nitrobenzoic acid) (DTNB) (Ellman's reagent) by sulfhydryl groups to 2-nitro-5-mercaptobenzoic acid, which has an intense yellow color. The results were expressed in mg per g protein (mg g^{-1} protein). The hepatic protein levels were determined spectrophotometrically at 595 nm using Coomassie Blue G 250 as a protein binding dye [24]. Bovine serum albumin was used as a protein standard.

2.6. Nuclease-like activity assay

Genomic deoxyribonucleic acid (DNA) was extracted from mammalian blood by salting out method [25] to examine the DNA cleavage activity of examined complexes. DNA purity and concentration were examined spectrophotometrically at 260/280 nm. The cleavage reactions were carried out in a total volume of 15 μ L containing 5- μ L genomic DNA, 5- μ L copper(II) complex (from 1.0 mM to 10.0 mM), and 5 μ L-buffer (25-mM Tris–HCl containing 50-mM NaCl pH 7.2). Genomic DNA alone, genomic DNA plus buffer, and buffer only were used as controls. The reactions were carried out at 37 °C at different time points (0, 1, 2, 4, 6, 12, and 24 h). A solution of loading dye (0.05% bromophenol blue, 5% glycerol, and 2 mM EDTA) was added to the reaction mixtures prior to gel running. Dose- and time-dependent experiments were carried out for each complex used in this study. Examined complexes were run on 1% agarose gel at a constant voltage of 100 V for 30 min in Tris-Borate- EDTA (TBE) buffer. Gels were stained with ethidium bromide and visualized under an ultraviolet (UV) transilluminator (Syngene gel documentation system) and photographed using a digital camera. Modified salting-out method that gave high-yield and high-quality genomic DNA from whole blood using laundry detergent was used [26].

3. Results and discussion

3.1. Characterization of the copper(II) complexes 1–4

The syntheses of copper(II) complexes $[\text{Cu}(\text{Albz})(\text{H}_2\text{O})_2](\text{ClO}_4)_2$ (**1**), $[\text{Cu}(\text{Albz})_2(\text{Cl})]\text{Cl}\cdot 2\text{H}_2\text{O}$ (**2**), $[\text{Cu}(\text{Albz})_2(\text{NO}_3)](\text{NO}_3)$ (**3**), and $[\text{Cu}_2(\text{Albz})_2(\mu\text{-SO}_4)_2(\text{H}_2\text{O})_2]$ (**4**) (scheme 1) were carried out by heating equimolar amounts of Albz with the corresponding copper(II)

Table 1. Molecular formulas, elemental analyses, and physical properties of **1–4**.

Compound	Found (Calc.)%							
	Yield g (%)	%C	%H	%N	%Cl	%S	%Cu	Λ_M ($\Omega^{-1}\text{cm}^2\text{mol}^{-1}$)
$[\text{Cu}(\text{Albz})(\text{H}_2\text{O})_2][(\text{ClO}_4)_2\text{C}_{12}\text{H}_{19}\text{Cl}_2\text{N}_3\text{O}_{12}\text{SCu}]$ (1)	0.406 (72%)	26.23 (25.56)	3.55 (3.40)	7.38 (7.45)	12.41 (12.58)	5.78 (5.63)	11.19 (11.27)	150.5
$[\text{Cu}(\text{Albz})_2\text{Cl}][\text{Cl}\cdot 2\text{H}_2\text{OC}_{24}\text{H}_{34}\text{Cl}_2\text{N}_6\text{O}_6\text{S}_2\text{Cu}]$ (2)	0.442 (63%)	41.98 (41.11)	4.67 (4.89)	9.96 (10.11)	12.31 (11.99)	9.01 (9.15)	9.28 (9.06)	89.5
$[\text{Cu}(\text{Albz})_2](\text{NO}_3)[(\text{NO}_3)\text{C}_{24}\text{H}_{30}\text{N}_8\text{O}_{10}\text{S}_2\text{Cu}]$ (3)	0.424 (59%)	39.87 (40.14)	3.98 (4.21)	15.82 (15.60)	—	8.52 (8.88)	8.59 (8.80)	115.9
$[\text{Cu}_2(\text{Albz})_2(\mu\text{-SO}_4)_2(\text{H}_2\text{O})_2]\text{C}_{24}\text{H}_{34}\text{N}_6\text{O}_{14}\text{S}_4\text{Cu}_2$ (4)	0.488 (68%)	33.29 (32.54)	3.64 (3.87)	9.77 (9.49)	—	14.13 (14.48)	15.09 (14.35)	35.5

salts in absolute methanol for 3 h. Chemical analysis and some physical properties of the isolated pure copper(II) complexes are listed in table 1. The analytical results demonstrate that **1** and **4** have 1 : 1 copper(II) : ligand stoichiometry, whereas **2** and **3** have 1 : 2 copper (II) : ligand ratios. The microcrystalline complexes are stable as solids or in solution under atmospheric conditions. The molar conductivity data for *ca.* 10^{-3} M $[\text{Cu}(\text{Albz})_2\text{Cl}]\text{Cl}\cdot 2\text{H}_2\text{O}$ (**2**) and $[\text{Cu}(\text{Albz})_2(\text{NO}_3)](\text{NO}_3)$ (**3**) in DMF at room temperature are in accord with those

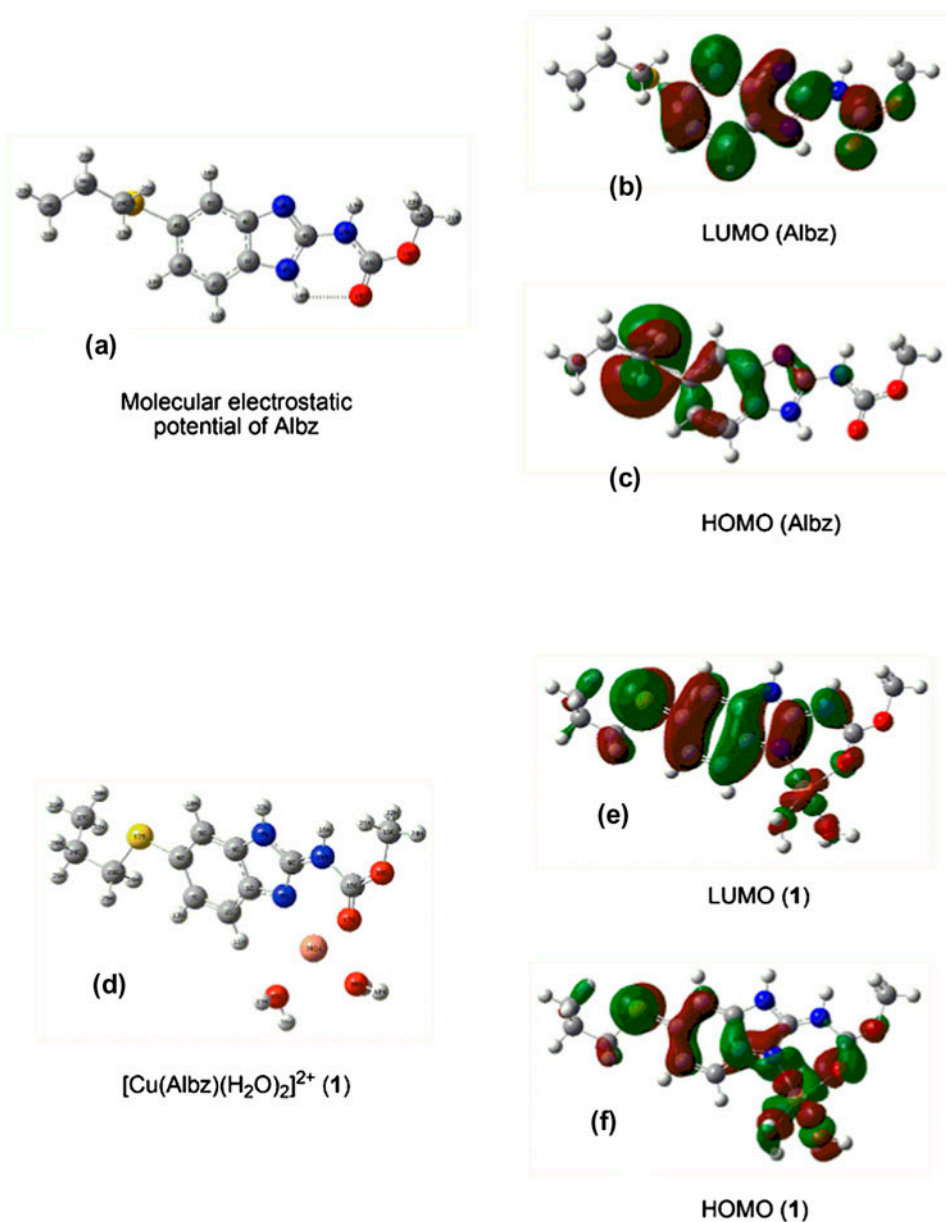


Figure 1. HOMO and LUMO orbitals with energy of Albz and **1** obtained from B3LYP/6-311 + G(d,p) method.

expected for a 1 : 1 electrolyte [27], while the measured value for perchlorate complex under the same conditions is as expected for a 1 : 2 electrolyte. These observations imply that one of the anions in chloro and nitrate complexes is coordinated to copper(II), while the perchlorate in $[\text{Cu}(\text{Albz})(\text{H}_2\text{O})_2](\text{ClO}_4)_2$ does not participate in coordination. For the bridging sulfate complex $[\text{Cu}_2(\text{Albz})_2(\mu\text{-SO}_4)_2(\text{H}_2\text{O})_2]$ (**4**), the low electrical conductance in solution indicates its non-electrolytic nature, suggesting that the sulfate groups are bridges in a dimeric structure (scheme 1). This conclusion is further supported by the results of IR spectra, ESR spectra, and the magnetic moment measurements.

3.2. Geometry optimizations and structure characterization

The optimized geometry of Albz is shown in figure 1(a). Calculations with DFT at B3LYP/6-311 + G(d,p) show that uncomplexed Albz is stabilized by hydrogen bond formation between the H14 and O18 (2.07 Å, O18-H14-N8 = 120°). Frontier orbital calculations, using TD-DFT method at B3LYP/6-311 + G(d,p), show that the HOMO orbitals [figure 1(c)] are positioned at S, while the LUMO orbitals [figure 1(b)] are distributed over the benzimidazole. The current distribution of HOMO-LUMO orbitals is not favored for complexation of Albz with metal ions, hence, upon complexation of Albz with Cu(II), the carbonyl group (C=O) rotates by 180° [figure 1(d)]. The bond length between Cu and N is 2.04 Å (30.8% less than the sum VDW radius), while the bond length between Cu and O is 2.08 Å (28.8% less than the sum of VDW radius). Cu is covalently bonded to two water ligands, equally separated from O_w (2.07 Å). The HOMO orbitals of Albz-Cu(II) complex are centered at Cu, while the LUMO orbitals are distributed over the Albz-Cu(II) complex.

3.3. Infrared spectra of 1–4

The most important bands occurring in IR spectra of free Albz and its copper(II) chelates have been compared to ascertain the bonding sites in the chelating ligand (table 2). The IR spectrum of the ligand exhibits bands at 3328 cm^{-1} and *ca.* 1460 cm^{-1} , assigned to $\nu(\text{NH})$ stretching and $\delta(\text{NH})$ bending of the benzimidazole ring, respectively [28]. The spectrum of the free ligand also exhibits bands at 1710 cm^{-1} , 1617 cm^{-1} , and 1007 cm^{-1} attributed to $\nu(\text{C}=\text{O})$, $\nu(\text{C}=\text{N})$, and the $\nu(\text{C}-\text{S})$, respectively. The effect of copper(II) binding on the

Table 2. The characteristic IR bands of Albz and 1–4.

Albz	1	2	3	4	Assignments
-	3523	3489	-	3508	O-H _{water}
3328	3275	3395	3225	3275	N-H st.
2966	2871	3125, 2967	2960	2871	C-H _{aliph} st.
1710	1677	1680	1670	1676	C=O st.
1617	1631	1631	1635	1629	C=N st.
1586	1584	1582	1578	1580	C=C st.
1460	1450	1443	1451	1449	N-H _{amide} Def.
1059	1048	1044	1045	1046	C-N=C ben.
-	-	-	1293, 802	-	$\nu(\text{N}=\text{O})$
-	1039, 762	-	-	-	ClO_4^-
1007	969	967	968	959	C-S st.
611	618	599	615	601	C-H Obp.
-	428	423	425	421	Cu-N st.
-	433	431	238	235	Cu-O st.

ring vibration of C-C = N-C in the benzimidazole ring of the ligand system has been investigated. The observed bands at 1631–1629 cm⁻¹, ~1048 cm⁻¹, and 601–618 cm⁻¹ for **1–4** (Supplementary Material S1) were assigned as ring stretching, ring bending, and ring out-of-plane deformation, respectively [21–26]. These bands were shifted by ~13, ~11, and ~8 cm⁻¹ to lower frequencies upon coordination to copper(II). These spectral features denote that coordination of Albz takes place through the sp² hybridized nitrogen of benzimidazole and carbonyl oxygen (scheme 1). This mode of bonding to copper(II) ion is further supported by the appearance of new absorption bands at 420–428 cm⁻¹ and 431–438 cm⁻¹, which are not observed in the spectrum of the free ligand. These bands are assignable to ν (Cu-N) and ν (Cu-O) [27]. The spectrum of **1** (figure 1) shows very intense absorption bands at 1039 cm⁻¹ and 762 cm⁻¹, which indicate the ionic character of ClO₄⁻ [21]. Complex **3** exhibits vibrational frequencies characteristic of both uncoordinated and coordinated nitrate; a very strong band at ~1293 cm⁻¹ assignable to ν (N = O) of the coordinated nitrate group of C_{2v} symmetry and two bands at 1381 cm⁻¹ and 802 cm⁻¹ attributed to the ν_3 and ν_2 vibrations, respectively, of ionic nitrate of D_{3h} symmetry [21]. The spectrum of the bridged sulfate complex **4** has a split band at 1175 cm⁻¹, 1116 cm⁻¹, and 1025 cm⁻¹. This band is assignable to the ν_3 frequency of sulfate; ν_4 , however, appears as a strong band at 619 cm⁻¹. This behavior is indicative of a bidentate SO₄ group of C_{2v} symmetry [21], and the absence of a band around 1250 cm⁻¹ suggests that this group is bridging rather than chelating [28]. Therefore, in this complex, copper(II) is probably five-coordinate with two sulfate groups bridging two [Cu(Albz)(H₂O)] units to give the dimeric complex, [Cu₂(Albz)₂(μ -SO₄)₂(H₂O)₂] (**4**) [29]. In the -OH stretching region, a very broad absorption extending from about 3320 to 3350 cm⁻¹ is detected for lattice and coordinated water in **1**, **2**, and **4** [30]. The water coordinated as a true ligand in the inner sphere of the copper(II) ion in these complexes can be recognized in the IR spectra by the appearance of wagging, twisting, and rocking bands of the Cu-OH₂ structural unit, established by coordination to the metal ion. For **1** and **4**, a rocking vibration appears at 890 cm⁻¹, a wagging vibration at 750 cm⁻¹, and the metal–oxygen stretch at 670 cm⁻¹.

3.4. Electronic absorption spectra

Electronic absorption spectra of the reported copper(II) complexes were recorded in DMF solutions at room temperature and the obtained results are tabulated in table 3. Figure 2 shows that electronic absorption spectral features of the five-coordinate **2**, **3**, and **4** are all similar. In square-pyramidal copper(II) complexes, the plausible d-orbital energy level scheme (idealized symmetry group C_{4v}) is $d_{x^2-y^2} > d_z^2 > d_{xy} > d_{xz}, d_{yz}$ [31]. Accordingly, the electronic spectra of five-coordinate copper(II) complexes in square-pyramidal geometry

Table 3. Electronic absorption spectra (cm⁻¹) of **1–4**.

*Complex	λ_{max} (cm ⁻¹)		
1	${}^2B_{1g} \rightarrow {}^2B_{2g}$	${}^2B_{1g} \rightarrow {}^2A_{1g}$	${}^2B_{1g} \rightarrow {}^2E_g$
	14,084	15,625	18,181
2	$d_{xy} \rightarrow d_{x^2-y^2}$	$d_{xz}, d_{yz} \rightarrow d_{x^2-y^2}$	
	16,393	18,518	
3	16,806	18,518	
4	16,949	18,348	

*Complex details are as listed in table 1.

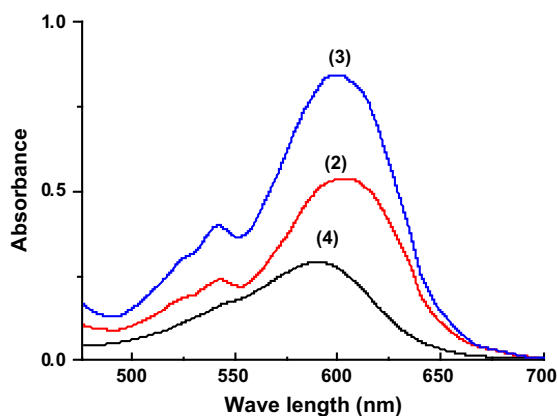


Figure 2. Electronic absorption spectra of **2**, **3**, and **4**.

will show three d–d bands [31], assigned to the transitions $d_z^2 \rightarrow d_{x^2-y^2}$, $d_{xy} \rightarrow d_{x^2-y^2}$, and $d_{xz}, d_{yz} \rightarrow d_{x^2-y^2}$. The spectra of **2–4** show two bands at $16,393 - 16,949 \text{ cm}^{-1}$ and $18,348 - 18,518 \text{ cm}^{-1}$, assigned to the $d_{xy} \rightarrow d_{x^2-y^2}$ and $d_{xz}, d_{yz} \rightarrow d_{x^2-y^2}$ transitions, respectively. Because of the low intensity of the $d_z^2 \rightarrow d_{x^2-y^2}$ transition, this band is usually not observed as a separate band in tetragonally distorted complexes. The electronic absorption spectra of the four-coordinate perchlorate complex **1** (Supplementary Material S2) displayed three d–d transitions at $14,084 \text{ cm}^{-1}$, $15,625 \text{ cm}^{-1}$ and $18,181 \text{ cm}^{-1}$, assignable to $^2B_{1g} \rightarrow ^2B_{2g}$, $^2B_{1g} \rightarrow ^2A_{1g}$ and $^2B_{1g} \rightarrow ^2E_g$ transitions, respectively [31]. The geometries of these copper(II) complexes under investigation is supported by magnetic measurements.

3.5. ESR spectra and magnetic moment studies

The magnetic susceptibility measurements at room temperature in the solid state show that the present complexes are paramagnetic. The observed magnetic moment values of **1–3** are $1.79 - 1.82 \text{ B.M.}$ [32, 33], indicating monomeric complexes with no exchange interaction between neighboring copper(II) ions in the polycrystalline state. This finding is further confirmed from the clear resolution of the ESR spectra. The observed magnetic moment per metal ion in **4** (table 4) is lower than the spin-only value for $S = 1/2$ usually observed in the absence of any exchange interaction. This lowering at room temperature reveals the presence of some spin-exchange interaction between the two copper(II) centers in the dimeric structure (scheme 1). In this complex, the bridged copper ions can have an appreciable

Table 4. Magnetic moment values and ESR spectral data of **1–4**.

*Complex	$(g_{\parallel})g_z$	g_y	$(g_{\perp})g_x$	R	g_{av}	G	$\mu_{eff} \text{ (BM)}$
1	2.449		2.109		2.222	4.119	1.81
2	2.453	2.265	2.110	0.824	2.224	4.118	1.79
3	2.438	2.260	2.108	0.853	2.218	4.056	1.82
4	2.430	2.255	2.115	0.800	2.220	3.739	1.52

*Complex details are as listed in table 1.

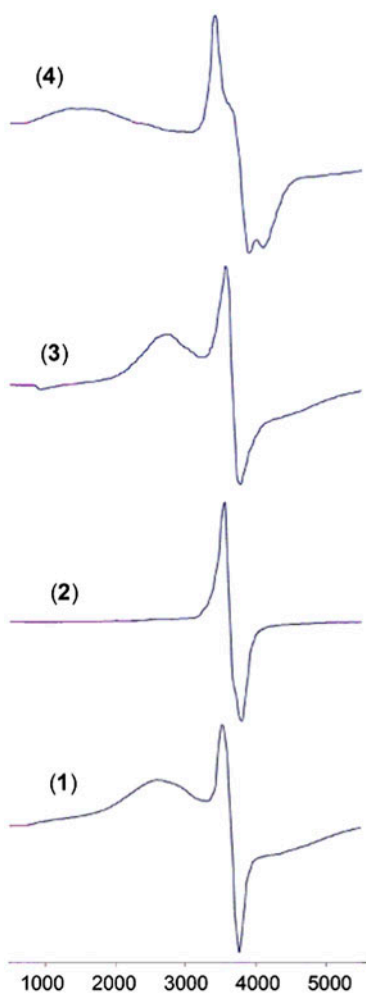


Figure 3. ESR spectra of **1**–**4**.

spin-exchange interaction, decreasing the magnetic moment. This is also supported by ESR spectral results, which give G -value lower than four for **4** and higher than four for the other complexes.

The X-band ESR spectra (figure 3) of polycrystalline samples of the synthesized copper (II) complexes were recorded at room temperature. The g_{\parallel} and g_{\perp} values were computed from spectra using DPPH ($g = 2.0027$) as “ g ” marker. Based on the g -values (table 4), the copper(II) ion in **1** is in an axial distorted ligand field [32, 33], characteristic of axial symmetry with elongation of axial bonds and the orbital $d_{x^2-y^2}$ as the ground state. Elongated square planar or distorted square-pyramidal stereochemistries would be consistent with these data, but trigonal-pyramidal involving compression of the axial bonds can be excluded [34]. The ESR parameters and the electronic transition energies of **1** are comparable with that reported for analogous copper(II) complexes containing four-coordinate copper(II) centers in a square-planar stereochemistry [35–37].

The five-coordinate **2–4** show parameters which are characteristic of rhombic symmetry. For systems with $g_z > g_y > g_x$ the parameter R ($R = (g_x - g_y)/g_z - g_y$) is very useful. If the ground state is d_{z^2} , the value of R is higher than 1, and the geometry of copper(II) ion is trigonal-bipyramidal; for the ground state being predominantly $d_{x^2-y^2}$, the value of R is lower than 1.0. Complexes **2–4** show values of R (table 4) lower than 1.0, indicating five-coordinate square-pyramidal geometry. The ESR data obtained for the complexes, together with the position of the d–d absorption bands, point out to a square-pyramidal structure [35–37].

The g_z and g_x values are equivalent to g_{\parallel} and g_{\perp} , respectively, and the g_{av} value is given by $g_{av} = (g_{\parallel} + 2 g_{\perp})/3$ [33]. The observed g_{av} values of the reported copper(II) complexes (table 4) are lower than 2.3; consequently, the coordination environment is covalent [38]. The value of the exchange interaction (G) between the copper(II) centers in a polycrystalline solid has been calculated using the relation $G = (g_{\parallel} - 2.0023)/(g_{\perp} - 2.0023)$ [39]. According to Hathaway *et al.* if the $G > 4$, the exchange interaction is negligible, while $G < 4$ indicates considerable exchange interaction in the solid complexes [39]. The data in table 4 reflect the absence of any exchange interaction between copper(II) centers in the monomeric solid complexes in accord with the results of magnetic moment measurements. On the other hand, the calculated G value (3.739) of dimeric **4** is lower than 4, indicating the presence of an appreciable spin-exchange interaction between the two copper(II) centers in the solid state, in agreement with the results of the magnetic susceptibility measurements of this complex.

3.6. Thermo-analytical studies

The thermal analysis measurements indicate that decomposition of **2–4** proceeds in several stages. The TG-DTA thermogram of **2** (Supplementary Material S3) exhibits an exothermic event at 375 K accompanied by a mass loss of 5.06% (calc. 5.13%), assigned to the removal of two lattice water molecules. This process is followed by two decomposition processes as evidenced by the strong exothermic and endothermic events at 488 K and 573 K, respectively, and are accompanied by a total mass loss of 49.70% (calc. 50.61%). This is due to loss of two chlorides and two Albz, forming a mixture of Cu_2C_2 and Cu_2S_2 as a final solid product (found 45.19%; calc. 44.26%). The pyrolysis of **3** (Supplementary Material S3) showed that the complex is stable to 428 K and then continuous mass loss occurs from 444 to 684 K. The endothermic event at 430 K accompanied by a mass loss of 42.28% (calc. 42.43%) is assigned for elimination of two nitrates and 40% of Albz. Another endothermic peak at 550 K, from the decomposition of the remaining Albz moieties (found 15.12%; calc. 15.98%), forms a mixture of Cu_2C_2 and Cu_2S as a final solid (found 41.98%; calc. 43.17%). The thermal decomposition of **4** (Supplementary Material S3) consists of several steps between 363 K and 773 K, due to the removal of the two coordinated waters and two Albz ligands, forming a mixture of Cu_2C_2 and Cu_2S_2 as a final solid product (found 38.85%; calc. 38.66%).

3.7. Electrochemical studies

The electrochemical behavior of Albz was carried out using CPE as the working electrode, Ag/AgCl as reference electrode, and platinum wire as auxiliary electrode, in the presence of 0.03 M KCl as supporting electrolyte using cyclic voltammetry. Cyclic voltammogram

shows two oxidation peaks at 0.824 V and 1.03 V, and no reduction peaks. The electrochemical behavior of **1** (Supplementary Material S4) using the previous conditions shows in addition to the previous oxidation peaks of the ligand two reduction peaks at 0.983 V and 1.26 V. These reduction peaks are from the copper complex. **2**, **3**, and **4** show the same trend as indicated in the figures of their cyclic voltammograms (Supplementary Material S4). Taking into account the reduction potential of the couples O_2^-/O_2^{2-} and O_2/O_2^- (+0.98 V and -0.45 V, pH 7, respectively) [40], any redox pair with a potential between these limits can act as a catalyst for antioxidation reactions. The observed redox potential values ($E_{1/2}$) of the reported copper(II) complexes lie in the middle of this range. Therefore, the electrochemical behavior observed for the investigated copper(II) complexes is in agreement with the results of the antioxidant activity.

3.8. Toxicity studies

Toxicity parameters including LD₅₀, GPT, and LDH activities were determined in normal limits compared to infected untreated group with concentrations up to 1000 mg kg⁻¹ b. wt. The GPT, an enzyme which allows determining the liver function as indicator on liver cells damage and LDH enzyme, is often used as a marker of tissue breakdown [41].

3.8.1. Evaluation of antioxidant activity. The protective effects of synthesized compounds against (CCl₄)-induced acute hepatotoxicity in mice were evaluated. CCl₄-induced hepatic injury has been extensively used in animal models to evaluate the therapeutic potential of drugs and dietary antioxidants [42–44]. CCl₄-induced trichloromethyl free radicals are capable to bind with DNA, lipids, proteins, or carbohydrates and eventually lead to membrane lipid peroxidation and finally to cell death [45, 46]. Hepatic GSH-Rd, serum activities of SOD and GST levels were measured to monitor liver injury and monitor the antioxidant activity. The results are presented in figure 4. SOD and GSH-S-transferase are known to protect cells from oxidative stress of highly reactive free radicals. Complexes **1**

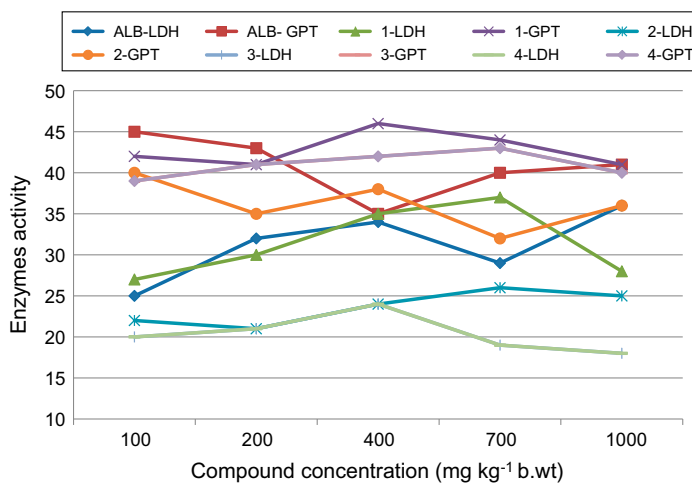


Figure 4. Effects of **1–4** on activities of GPT and LDH enzymes.

and **2** have higher antioxidant activities as compared to standard antioxidant (vitamin E) [47, 48]. The results indicate that significantly lower activities ($p < 0.05$) of SOD, GST, and GSH-Rd were observed in CCl_4 -treated group as compared to the normal control group. Also, there was significant restoration ($p < 0.05$) in SOD and GST activities in the treated groups at doses of 100 and 300 mg kg^{-1} for the treated group 2. The reduction of SOD, GST, and GSH-Rd activities by copper(II) complexes were compared to the CCl_4 -treated control group ($p < 0.05$). No significant difference was found between used doses (100 and 300 mg kg^{-1}) with all tested compounds. On the other hand, the highest restoration in SOD and GST, activities rather than GSH-Rd levels were monitored with **1** and **2** as compared to group 2. The reduction of SOD, GST, and GSH-Rd activities by the copper(II) complexes is an indication of repair of hepatic tissue damage induced by CCl_4 . This is in agreement with Thabrew *et al.* [49] who found that serum transaminases returned to normal activities with the healing of hepatic parenchyma and regeneration of hepatocytes. Thus, administration of these copper(II) systems revealed hepatoprotective activity against the toxic effect of CCl_4 .

Oxidative stress induced due to the generation of free radicals and/or decreased antioxidant level in the target cells and tissues has been suggested to play an important role in carcinogenesis [50]. During cell membrane damage, various enzymes leak down to the circulatory fluid and their assessment in serum serves as markers in clinical studies. SOD is the first antioxidant enzyme to deal with oxyradicals by accelerating the dismutation of superoxide to hydrogen peroxide. Thus, SOD acts as a supportive anti-oxidative enzyme, providing protective defense against reactive oxygen species [51]. The present study reveals that SOD, GST, and GSH-Rd activities decreased in CCl_4 injected animal, which may be due to altered antioxidant status.

The probable mechanism of the superoxide disproportionation catalyzed by **1–4** may proceed similarly. The interaction mechanism (scheme 2) could involve direct attack of O_2^- on the free axial position of the copper(II) ion for the five-coordinate square-pyramidal **2** passing through a six-coordinate adduct, which is highly unstable due to Jahn–Teller effect [52]. As a consequence of this interaction, copper(II) undergoes rapid reduction to copper(I) with the release of O_2 . Electron transfer between the central metal and O_2^- occurs by direct binding [53]. According to the electroneutrality principle [54], the electronegativity of the coordinated various anions in complexes plays a significant role in the value of the formal charge of the copper(II) ion, which consequently affects the redox potential of $\text{Cu}^{2+}/\text{Cu}^+$. At this stage, probably because of the tetrahedral preference of copper(I), the axial coordinated anion could be dissociated from the complex in solution. In a fast reaction, the tetrahedral copper(I) is reoxidized to copper(II) by a second O_2^- with concomitant formation of peroxide dianion O_2^{2-} . The protonation of O_2^{2-} prior to its release from the complex is required, because the peroxide dianion is highly basic and thus too unstable to be released in unprotonated form. The proton can then coordinate to the coordinatively unsaturated peroxo-copper(II) complex, which rearranges to give the perhydroxyl radical $\text{H}_2\text{O}^\bullet$. The basic perhydroxyl (hydroperoxide) formed is further protonated as a result of electrophilic attack by proton on the oxygen-bonded copper(II) with release of H_2O_2 and regeneration of the catalyst in its original active form. The reaction sequence for the catalytic disproportionation of O_2^- by copper(II) complexes may therefore be represented as shown in scheme 2.

3.8.2. Nuclease-like activity. DNA is an important substrate for hydrolytic cleavage. Because of its polyanionic nature, DNA is resistant to hydrolysis. Super-coiled (SC) plasmid DNA, which is commonly observed in bacterial cells, is a cyclic super-coiled

double-strand made up of several thousand base pairs. By coordinating to this substrate, metal ions serve as Lewis acids to activate the phosphodiester for nucleophilic attack. The metal-coordinated water M-OH species acts as a nucleophile to attack the SC DNA form (I). Then SC DNA is relaxed to nicked circular form (II) and further cleaved to linear form (III). When subjected to electrophoresis, relatively fast migration is observed for form (I), slower migration for form (II), and form (III). The characterization of DNA recognition by transition metal complexes have been aided by the DNA cleavage chemistry that is associated with redox-active or photoactivated metal complexes [55]. The nuclease-like activity of **1** and **2** was investigated under aerobic conditions at room temperature and in the absence of external additives (figure 5). The experimental observations demonstrated that **1** has promising ability towards cleavage of genomic DNA in both dose- and time-dependent manner. The nuclease-like activity was correlated with the increments of the concentration (0–10 mM) and time (0–24 h) as shown in figure 5 (middle panel) and figure 6.

DNA cleavage was analyzed by monitoring the conversion of SC DNA to nicked DNA and linear DNA at 37 °C. Complex **1** can cleave the SC DNA to nicked and linear DNA at the same time. As shown in figure 5, with increase in dose of **1** as a representative example, the intensity of the circular SC DNA band decreased, while that of nicked and linear DNA bands increase. When the complex concentration was 10 mM (middle panel), the circular SC DNA band disappeared completely. Due to the labile coordination sphere, copper(II) complexes have attracted special attention as endonuclease mimics. Different mechanisms for DNA cleavage have been assumed, including hydrolytic or oxidative pathways. Complex **2** did not show DNA nuclease-like activity in dose effect as seen in figure 5 (lower panel). Hydrolytic cleavage directly breaks the phosphodiester bond, but does not result in sugar damage [56, 57]. The phosphatodiester backbone of DNA is very stable and resistant to hydrolytic cleavage. Copper(II) complexes of linear or macrocyclic polyamines, aminoglycosides, and histidine show good nuclease activity [56, 58]. This result is in accord with that recently discovered for analogous copper(II) complexes that catalytically cleave target DNA in the absence of any external reductant. However, this action proceeds by attacking multiple positions of the nucleotide, indicating that the DNA cleavage reaction is oxidative through a non-diffusible radical mechanism [59]. The present study demonstrates that **1** has significant nuclease activity towards cleavage of genomic DNA in the absence of external additives. Its easy preparation and DNA cleavage activity without any additive make it a promising complex for anticancer activity.

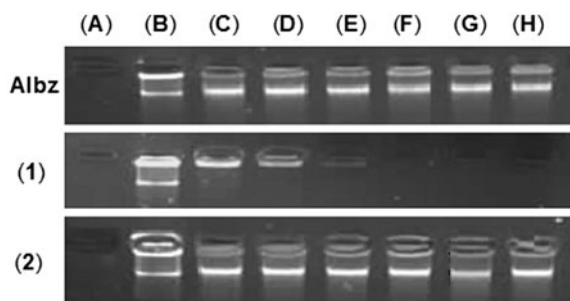


Figure 5. Dose-dependant effect of Albz, **1**, and **2** on DNA cleavage and binding activity. Copper(II) complexes were incubated with genomic DNA : (A) buffer; (B) genomic DNA; (C) 1 mM; (D) 2 mM; (E) 4 mM; (F) 6 mM; (G) 8 mM; and (H) 10 mM at 37 °C for 24 h. DNA was electrophoresed in 1% agarose gel stained with ethidium bromide for 30 min and photographed on a Syngene gel documentation system.

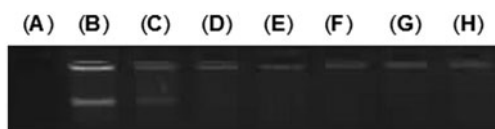
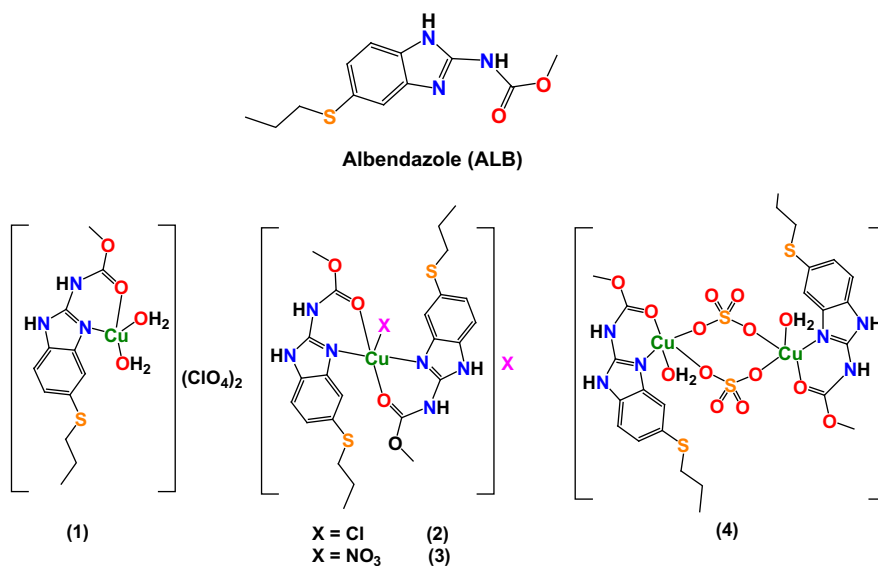
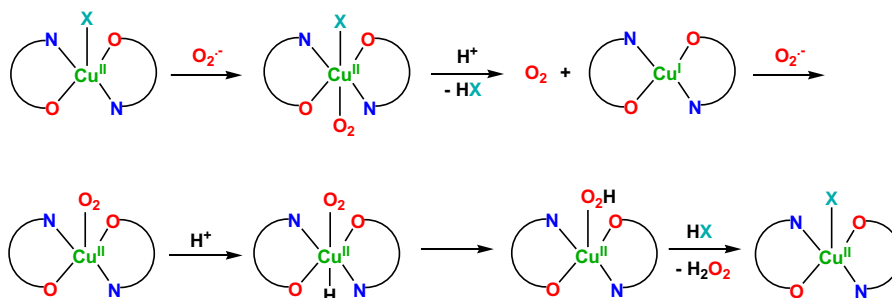


Figure 6. Time dependant effect of **1** on DNA binding activity. **1** in a dose of 4 mM was incubated with genomic DNA : (A) buffer; (B) 0 h; (C) 1 h; (D) 2 h; (E) 4 h; (F) 6 h; (G) 12 h; and (H) 24 h at 37 °C. Reaction contents were electrophoresed in 1% agarose gel stained with ethidium bromide for 30 min and photographed on a Syngene gel documentation system.



Scheme 1. The structure of Albz and **1-4**.



Scheme 2. The reaction sequence for the catalytic disproportionation of $\text{O}_2^{\bullet -}$ by **2**.

4. Conclusion

A series of albendazole-based copper(II) complexes, $[\text{Cu}(\text{Alb})(\text{H}_2\text{O})_2](\text{ClO}_4)_2$ (**1**), $[\text{Cu}(\text{Albz})_2(\text{Cl})]\text{Cl}\cdot 2\text{H}_2\text{O}$ (**2**), $[\text{Cu}(\text{Albz})_2(\text{NO}_3)](\text{NO}_3)$ (**3**), and $[\text{Cu}_2(\text{Albz})_2(\mu\text{-SO}_4)_2(\text{H}_2\text{O})_2]$ (**4**) (Albz = albendazole), have been synthesized and fully characterized. Complex **1** is proposed to be square-planar, whereas square pyramidal geometry is suggested for **2–4**. Quantum mechanics (QM) calculations using B3LYP/6–311 + G(d,p) level of theory corroborated the experimental results to investigate the building and geometry optimization of the ligand Albz and **1**. The hepatoprotective and antioxidative efficacy of Albz and **1–4** were evaluated against CCl_4 -induced acute hepatotoxicity in experimental rats. The results show significant decrease in the antioxidant enzyme activities (SOD, GSH-S-transferase, and GSH-Rd levels). The cleavage activity of super-coiled DNA was ascertained by gel electrophoresis mobility assay. Complex **1** is effective in the cleavage of plasmid super-coiled form (I) and consequently resulting nicked circular form (II) of DNA.

Disclosure statement

No potential conflict of interest was reported by the authors.

Funding

This work was supported by Taif University, Saudi Arabia [project number 1/1434/2695].

Supplemental data

Supplemental data for this article can be accessed <http://dx.doi.org/10.1080/00958972.2015.1093124>.

References

- [1] G. Singh, S. Maurya, M.P. deLampasona, C.A.N. Catalan. *Food Chem. Toxicol.*, **45**, 1650 (2007).
- [2] B. Halliwell, J.M.C. Gutteridge (Eds.). *Free Radicals in Biology and Medicine*, 3rd Edn, pp. 530–533, Springer, Berlin (1999).
- [3] L. Leong, G. Shui. *Food Chem.*, **76**, 69 (2002).
- [4] P.H. Proctor, J.E. McGinness. *Arch. Dermatol.*, **122**, 507 (1986).
- [5] A. Bhattacharya, A. Chatterjee, S. Ghosal, S.K. Bhattacharya. *Indian J. Exp. Biol.*, **37**, 676 (1999).
- [6] W. Peschel, F. Sánchez-Rabaneda, W. Diekmann, A. Plescher, I. Gartzia, D. Jiménez, R. Lamuela-Raventós, S. Buxaderas, C. Codina. *Food Chem.*, **97**, 137 (2006).
- [7] F. Shahidi, P.K. Janitha, P.K. Wanasundara. *Rev. Food Sci. Nutr.*, **32**, 67 (1992).
- [8] A.J. Kirby. *Angew. Chem. Int. Ed. Engl.*, **35**, 706 (1996).
- [9] M.M. Ibrahim, G.A.M. Mersal, S.A. Al-Juaid, S.A. El-Shazly. *J. Mol. Struct.*, **166**, 1056 (2014).
- [10] M.M. Ibrahim, G.A.M. Mersal, A.M. Ramadan, S.A. El-Shazly, M.A. Amin. *Int. J. Electrochem. Sci.*, **9**, 5298 (2014).
- [11] M.M. Ibrahim, A.M. Ramadan, G.A.M. Mersal, S.A. El-Shazly. *Int. J. Electrochem. Sci.*, **7**, 7526 (2014).
- [12] M.A. Ramadan, M.M. Ibrahim, I.M. El-Mehasseb. *J. Coord. Chem.*, **65**, 2256 (2012).
- [13] S.Y. Shaban, M.M. Ibrahim, F.W. Heinemann, R. Van Eldik. *J. Coord. Chem.*, **65**, 934 (2012).
- [14] M.A. Ramadan, M.M. Ibrahim, S.Y. Shaban. *J. Mol. Struct.*, **1006**, 348 (2011).
- [15] A.M. Ramadan, S.Y. Shaban, M.M. Ibrahim. *J. Coord. Chem.*, **64**, 3376 (2011).
- [16] K.D. Karlin, Z. Tyeklar. *Bioinorganic Chemistry of Copper*, Chapman & Hall, New York (1993).

- [17] M.N.Ghosh. *Fundamentals of Experimental Pharmacology*, 2nd Edn, p. 175, Scientific Book Agency, Kolkata (1984).
- [18] S. Reitman, S. Frankel. *Am. J. Clin. Pathol.*, **28**, 56 (1957).
- [19] H.U. Bergmeyer, *Methods of Enzymatic Analysis*, 2nd Edn, p. 534, Academic Press, New York, (1974).
- [20] S. Rai, A. Wahile, K. Mukherjee, B. Saha, P.K.Mukherjee. *J. Ethnopharmacol.*, **104**, 322 (2006).
- [21] W.H. Habig, M.J. Pabst, W.B. Jakoby. *J. Biol. Chem.*, **249**, 7130 (1974).
- [22] P. Kakkar, B. Das, P.N. Visvanathan. *Ind. J. Biochem. Biophys.*, **197**, 588 (1972).
- [23] G.L. Ellman. *Arch. Biochem. Biophys.*, **82**, 70 (1959).
- [24] M.M. Bradford. *Anal. Biochem.*, **72**, 248 (1976).
- [25] H. Nasiri, M. Forouzandeh, M.J. Rasaei, F. Rahbarizadeh. *J. Clin. Lab. Anal.*, **19**, 229 (2005).
- [26] S.S. Shams, S.Z. Vahed, F. Soltanzad, V. Kafil, A. Barzegari, S. Atashpaz, J. Bara. *BioImpacts*, **1**, 183 (2011).
- [27] W.J. Geary. *Coord. Chem. Rev.*, **7**, 81 (1971).
- [28] K. Nakamoto. *Infrared and Raman Spectra of Inorganic and Coordination Compounds*, p. 324, Wiley, New York (1986).
- [29] D.J. Rabiger, E. Joullié. *J. Org. Chem.*, **29**, 476 (1964).
- [30] H. Takeuchi, I. Harada. *Spectrochim. Acta*, **49**, 1069 (1986).
- [31] A.B.P. Lever. *Inorganic Electronic Spectroscopy*, Elsevier, Amsterdam (1970).
- [32] B.N. Figgis. *J. Lewis. Prog. Inorg. Chem.*, **6**, 37 (1964).
- [33] R.L. Dutta, A. Syamal. *Elements of Magnetochemistry*, 2nd Edn, Affiliated East-West Press, Delhi (2007).
- [34] A.S. Fernandes, J. Gaspar, M.F. Cabral, C. Caneiras, R. Guedes, M. Castro, J. Costa, N.G. Oliveira. *J. Inorg. Biochem.*, **101**, 849 (2007).
- [35] D.X. West, I. Thientaravanich, A.E. Liberta. *Transition Met. Chem.*, **20**, 303 (1995).
- [36] A.M. Ramadan, I.M. El-Mehasseb. *Transition Met. Chem.*, **23**, 183 (1998).
- [37] R. Sugich-Miranda, R.R. Sotelo-Mundo, E. Silva-Campa, J. Hernández, G.A. Gonzalez-Aguilar, E.F. Velazquez-Contreras. *J. Biochem. Mol. Toxicol.*, **24**, 379 (2010).
- [38] D. Kivelson, R. Neiman. *J. Chem. Phys.*, **35**, 149 (1961).
- [39] B.J. Hathaway, D.E. Billing. *Coord. Chem. Rev.*, **5**, 143 (1970).
- [40] B.V. Murdula, G. Venkatarayana, P. Lingaiah. *Indian J. Chem.*, **28A**, 104 (1989).
- [41] A.A. Butt, S. Michaels, D. Greer, R. Clark, P. Kissinger, D.H. Martin. *AIDS Read.*, **12**, 317 (2002).
- [42] Z. Taira, K. Yabe, Y. Hamaguchi, K. Hirayama, M. Kishimoto, S. Ishida, Y. Ueda. *Food Chem. Toxicol.*, **42**, 803 (2004).
- [43] K.J. Lee, J.H. Choi, H.G. Jeong. *Food Chem. Toxicol.*, **45**, 2118 (2007).
- [44] M. Rudnicki, M.M. Silveira, T.V. Pereira, M.R. Oliveira, F.H. Reginatto, F. Dal-Pizzol, J.C.F. Moreira. *Food Chem. Toxicol.*, **45**, 656 (2007).
- [45] L.W.D. Weber, M. Boll, A. Stampfl. *Crit. Rev. Toxicol.*, **33**, 105 (2003).
- [46] S. Basu. *Toxicology*, **189**, 113 (2003).
- [47] S.A. Ganie, B.A. Zargar, A. Masood, M.A. Zargar. *Biomed. Environ. Sci.*, **26**, 209 (2013).
- [48] S.M. Zaidi, T.M. Al-Qirim, N. Banu. *Drugs R&D*, **6**, 157 (2005).
- [49] M.I. Thabrew, P.D.T.M. Joice, W.A. Rajatissa. *Planta Med.*, **53**, 239 (1987).
- [50] Y.L. Huang, J.Y. Heu, T.H. Lin. *Clin. Biochem.*, **32**, 31 (1999).
- [51] C.J. Weydert, T.A. Waugh, J.M. Ritchie, K.S. Iyer, J.L. Smith, L. Li, D.R. Spitz, L.W. Oberley. *Free Rad. Biol. Med.*, **41**, 226 (2006).
- [52] F. Cotton, G. Wilkinson. *Advanced Inorganic Chemistry*, Wiley, New York (1972).
- [53] J.A. Fee, *Metal Ions in Biological Systems*, H. Sigel (Ed.), p. 13, Marcel Dekker, New York (1981).
- [54] J.E. Huheey, *Inorganic Chemistry Principles of Structure and Reactivity*, 3rd Edn, London (1983).
- [55] A.S. Sitlani, E.C. Long, A.M. Pyle, J.K. Barton. *J. Am. Chem. Soc.*, **114**, 2303 (1992).
- [56] C. Liu, M. Wang, T. Zhang, H. Sun. *Coord. Chem. Rev.*, **248**, 147 (2004).
- [57] F. Mancin, P. Scrimin, P. Tecilla, U. Tonellato. *Chem. Commun.*, 2540 (2005).
- [58] A. Bencini, E. Berni, A. Bianchi, C. Giorgi, B. Valtancoli, D.K. Chand. *Dalton Trans.*, 793 (2003).
- [59] P.U. Maheswari, S. Roy, H. den Dulk, S. Barends, G. van Wezel, B. Kozlevčar, P. Gamez, J. Reedijk. *J. Am. Chem. Soc.*, **128**, 710 (2006).